

Determination of Production Parameters of CuCrZr Alloy by Selective Laser Melting Process

*Makale Bilgisi / Article Info

Alındı/Received: 20.05.2024

Kabul/Accepted: 14.11.2024

Yayımlandı/Published: xx.xx.xxxx

CuCrZr Alaşımının Seçici Lazer Ergitme Prosesi ile Üretim Parametrelerinin Belirlenmesi

Burcu Aslı ÖZKAN^{1*}, Yusuf DİLSİZ¹, Cem ÖZATEŞ², Enes Furkan SEVİNÇ³, Cantekin KAYKILARLI¹, Cihan KABOĞLU¹, Deniz UZUNSOY¹

¹Bursa Technical University, Department of Metallurgical and Materials Engineering Faculty, Bursa, Türkiye

²Sentes Bir A.Ş., 35730, Kemalpaşa, İzmir, Türkiye

³Ermaksan Machinery Industry and Trade, 16065, Nilüfer, Bursa, Türkiye



Abstract

CuCrZr alloy is a widely preferred material in the space, defense, and electronics industries with its high thermal and electrical conductivity properties. There are limited publications investigating the tribological properties of CuCrZr alloys produced via the selective laser melting (SLM) method. In this study, it was aimed to optimize the process parameters and examine the effect of process parameters on density, hardness, microstructure, and tribological properties of domestically produced CuCrZr powder to be produced by the SLM method, which allows the production of complex structured parts. The optimum process parameters of the CuCrZr alloy were determined as laser power of 435 W, scanning speed of 350 mm/s, layer thickness of 0.02 mm, laser diameter of 0.1 mm, hatch distance of 0.1 mm, and energy density of 621.42 J/mm³. The relative density, hardness, COF, and wear values of the samples produced with the optimized SLM process parameters were obtained as 99.22% and 96 HV, 0.5520 ± 0.1648, and 1.17x 10⁻⁴ (mm³/Nm), respectively.

Anahtar Kelimeler: CuCrZr; Seçici lazer ergitme; Eklemeli imalat; Tribolojik davranış.

Öz

CuCrZr alaşımı, yüksek termal ve elektrik iletkenlik özellikleri ile uzay, savunma ve elektronik endüstrilerinde yaygın olarak tercih edilen bir malzemedir. SLM yöntemiyle üretilmiş olan CuCrZr alaşımının tribolojik özelliklerinin incelenmesi üzerine kısıtlı yayınlar mevcuttur. Bu çalışmada, yerli olarak üretilmiş olan CuCrZr tozundan, karmaşık yapıları parçaların üretimlerine olanak sağlayan seçici lazer ergitme (SLM) yöntemiyle üretilmek üzere proses parametrelerinin optimize edilmesi ve proses parametrelerinin yoğunluk, sertlik, mikroyapı ve tribolojik özellikleri üzerine etkisinin incelenmesi hedeflenmiştir. CuCrZr alaşımının optimum proses parametreleri lazer gücü 435 W, tarama hızı 350 mm/s, katman kalınlığı 0.02 mm, lazer çapı 0.1 mm, tarama aralığı 0.1 mm ve enerji yoğunluğu 621.42 J/mm³ olarak belirlenmiştir. Optimize edilen SLM proses parametreleriyle üretilen numunelerin relatif yoğunluk, sertlik, COF değeri ve aşınma değerleri sırasıyla % 99.22 ve 96 HV, 0.5520 ± 0.1648 ve 1.17x 10⁻⁴ (mm³/Nm) olarak elde edilmiştir.

Keywords: CuCrZr; Selective laser melting; Additive manufacturing; Tribological behaviors.

1. Introduction

Laser-based powder-bed fusion is a class of additive manufacturing processes that includes selective laser melting (SLM). This method builds up metal particles layer by layer to make a three-dimensional material by selectively melting and joining them with a powerful laser (Gokuldoss *et al.* 2017). The procedure is initiated by spreading a slender layer of metal powder across a construction platform. Following a pattern, a laser then sweeps over the powder bed, selectively fusing the particles by melting them. This action redifies the powder into a singular layer, contributing to the production of the designed three-dimensional part. The application of SLM technology is diverse and includes various fields, such as aerospace, automotive, medical,

and tooling industries. SLM is a desirable manufacturing process for components such as orthopedic implants, heat exchangers, turbine blades, circuit breakers, combustion chamber components, lightweight parts, and conformal cooling inserts because of its flexibility in design and capacity to create complex geometries (Tang *et al.* 2022, Yap *et al.* 2015, Zezhou *et al.* 2023, Salvan *et al.* 2021). One of the important advantages of SLM is its capability to produce parts from various materials, including high-performance alloys like titanium and nickel-based superalloys (Frazier 2014), and copper alloys. Especially the CuCrZr alloy is a precipitation-hardening alloy and has become important in many industries due to its high thermal and electrical conductivity combined with strong mechanical

properties (Wang *et al.* 2022). Sun *et al.* (2020) investigated the determination of process parameters of CuCrZr alloy and their effects on relative density. They reported that the effect of laser power on relative density is greater than the effect of scanning speed, and at the same laser power, scanning speed is more effective than scanning distance. Also, Özkan *et al.* (2024) used the taguchi and (ANOVA) analysis of variance statistical method to determine the process parameters of pure copper. In their study, it was reported that the most effective parameters for relative density were layer thickness, laser point size, and hatch distance, respectively. There is a little study on process optimization via applying remelting strategies. The process time is extended with the remelting application, but this can be ignored due to the improvements achieved in mechanical properties. Xu *et al.* (2024) applied the remelting process and investigated microstructure, mechanical properties, and conductivity performance. And good conductive CuCrZr alloy with a greater relative density and more consistent hardness was produced by the remelting method in comparison to the non-remelting specimens. Yaolong *et al.* (2024) found a link between porosity and laser power and encountered porosity problems at various rates. With the laser power operated at 480W, they obtained spherical pores in the range of 10–30 microns, and when the laser power was reduced to 375W, they observed that the pore size decreased, the amount of voids increased, and most of the pores were close to spherical.

Studies have shown that careful optimization of these parameters can lead to CuCrZr parts with mechanical properties comparable to or even surpass traditional fabricated parts. Prashanth *et al.* (2014), Xu *et al.* (2024), Prabu *et al.* (2024), Murugesan *et al.* (2024) investigated the tribological properties of partially molten particles with columnar, cellular, and equiaxed structures and defect-free surfaces of CuCrZr parts produced by the SLM method. The equiaxed structure showed higher wear resistance, and it was reported that the columnar grain structure had less wear resistance due to its fine structure. Fang *et al.* (2024) studied on process optimization of CuCrZr and investigated microstructure, mechanical properties and precipitates of CuCrZr alloys. They stated that fewer defects were obtained when 163 J/mm^3 laser energy density was applied. Zhangping *et al.* (2022) studied the effects of volumetric energy density (VED) among scanning parameters on relative density, microstructure, mechanical properties, and crystallographic texture. They found that excessively low

VED leads to a lack of fusion and unmelted powder, while excessively high VED leads to keyhole defect formation. In their research with pure copper, Yan *et al.* (2020) researched how linear energy density (laser power/laser scanning rate) affected the relative density and mechanical properties. They observed that when the linear energy density was lower (0.35 J/mm), unmelted powders and irregular pores were formed; when the linear energy density was 0.5 J/mm, there was a small amount of porosity; and when it exceeded 0.63 J/mm, large pores were formed. The studies in the literature researched the linear energy density parameter, or specifically each parameter, to achieve parameter optimization of CuCrZr alloy with the SLM method. In addition, a few studies have examined the wear properties of CuCrZr produced with SLM technology. In the production of CuCrZr alloy with the SLM method, a little study on the relationship between energy density and relative density expressed as the ratio (laser power/scanning speed x scanning distance x scanning speed) could be found in the known literature. In addition, this study is different from these studies in that the CuCrZr alloy powder is produced domestically, a remelting scanning strategy was applied and it investigates the relationship between energy density, relative density, hardness, and wear resistance.

This study was carried out with an infrared (IR) laser, and the laser power was fixed at 435 W. A remelting strategy was applied, and the highest density value was tried to be obtained by combining with other parameters. A comprehensive test evaluated key properties, including hardness, relative density, microstructure, and wear resistance. By systematically analyzing the results, the study identified correlations between processing conditions and material characteristics, leading to the optimization of production parameters. The study promises to pave the way for more efficient, precise, and cost-effective manufacturing processes, enhancing the applicability and performance of CuCrZr alloys across various industries.

2. Materials and Methods

In this research, CuCrZr alloy powders were produced using the gas atomization system developed by Sentas-BIR company. Gas atomization is a widely recognized manufacturing technique known for its ingenuity in producing spherical metal alloy powders with extraordinary properties, largely due to the rapid solidification phenomenon encountered during production. This method also yields alloy powders

characterized by reduced oxygen content, thus improving the overall quality of the resulting powders. However, it should be recognized that the particle size distribution of these powders typically covers the range of 1 μm to 1 mm. The atomization of CuCrZr began by alloying the desired components in an induction furnace, followed by pouring the molten alloy into the tundish. The gas pressure is carefully controlled under the atomization nozzle throughout the process. A precise adjustment of gas flow is achieved, as shown in Figure 1. (10-12bar). With this adjusted gas flow, powders with large grain sizes are obtained. This regulated gas flow facilitated the formation of particles covering a wide range of sizes. A schematic illustration of the CuCrZr powder atomization process is presented in Figure 1. To obtain the particle size distribution in the 15 to 45 μm range, an air classifier and a 45 μm screen were used. The intended outcome was attained by the selective retention and separation of particles within the designated size range made possible by this screening and classification process. An Ermaksan ENA 250 system (Ermaksan, Turkey) with a 500 W Yb-Fiber laser with a wavelength of 1064 nm, a laser spot size of 100 μm , and

a production volume of 250 mm x 250 mm x 300 mm was used to construct the SLM CuCrZr samples.

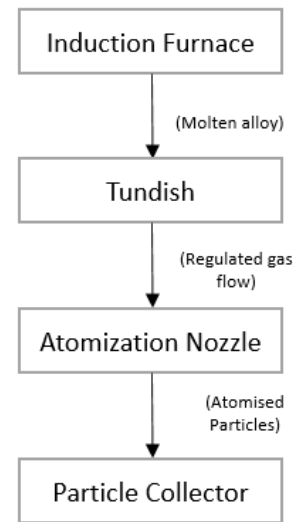


Figure 1. Schematic demonstration of the atomization process of CuCrZr alloy powder.

A schematic of the SLM CuCrZr alloy manufacturing process is shown in Figure 2. CuCrZr samples were treated in a high-purity argon environment to avoid material oxidation.

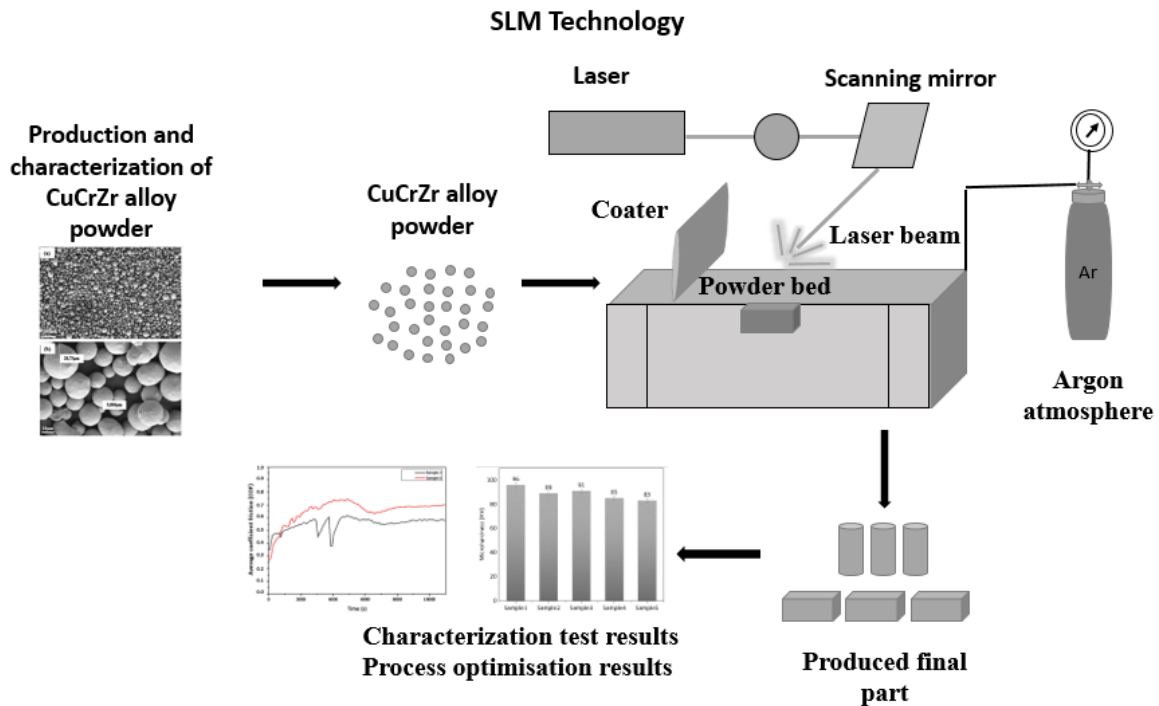


Figure 2. Schematic demonstration for the SLM production process of the CuCrZr alloy.

The oxygen content was kept below 2500 ppm in the chamber. To prevent the balling effect, a 316 L stainless steel substrate was preheated to 80 $^{\circ}\text{C}$. Due to its high thermal conductivity, the substrate needs to be heated between 80 $^{\circ}\text{C}$ and 120 $^{\circ}\text{C}$ to reduce heat dissipation and ensure better adhesion of the copper sample to the

substrate (Raab *et al.* 2016). A 67 $^{\circ}$ rotation angle between layers was used, and a zigzag and remelting scanning pattern was used. Energy density was calculated according to the formula given in Eq.1. Zaneta (2019).

$$E = \left(\frac{P}{vxhxt} \right) \quad (1)$$

where E (J/mm³) is the energy density, P (W) is the laser power, v (mm/s) is the scanning speed, h (mm) is the hatch distance and t (mm) is the layer thickness Zaneta (2019), Xu (2024).

Table 1 shows the process parameters that were used for this search.

Table 1. Process parameters of the study

Sample number	1	2	3	4	5
Laser Power (w)	435	435	435	435	435
Scanning speed (mm/s)	350	500	350	500	650
Layer thick. (mm)	0.02	0.02	0.03	0.03	0.03
Laser spot size (mm)	0.1	0.08	0.12	0.14	0.08
Hatch distance (mm)	0.1	0.09	0.10	0.09	0.08
Energy density (J/mm ³)	621	483	414	322	278

Figure 3 shows the image of cuboid samples processed by ENA 250 SLM printers. Characterization and test samples were produced with dimensions of 10 mm × 10 mm × 10 mm to determine relative density, microhardness, and wear resistance. The chemical composition of the powder is analyzed via X-ray fluorescence spectroscopy (XRF, Rigaku Supermini 200). Particle size analyzer equipment (Malvern Mastersizer 3000E), which is a liquid dispersion analysis method based on the principle of laser diffraction was used, and the analysis was performed according to the ASTM B822 standard to determine the size distribution of CuCrZr powders. Powder density measurement was done via a micrometric AccuPyc II 1340 gas pycnometer.

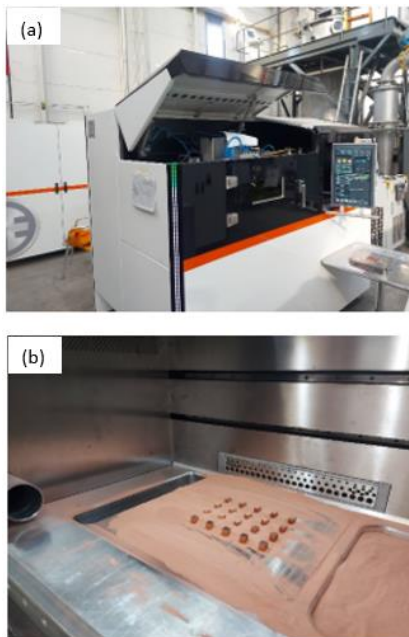


Figure 3. a) Image of produced cuboid parts via SLM process of CuCrZr alloy and b) ENA 250 SLM printer.

Figure 4 shows the powder density and powder flow ability testers. Apparent density measurement was done according to ASTM B212. Compressed density testing was performed via an auto-tapping denser (auto-tapping single station) according to ASTM B527. Additionally, to measure the flow ability of the CuCrZr powder, a hall flow test was performed with LPW brand equipment according to ASTM B213. Using Cu K α radiation ($\lambda = 1.5406 \text{ \AA}$, 40 kV, 40 mA, and 2θ range of 30–80°), X-ray diffraction (XRD, BrukerTM D8 Advanced Series Powder Diffractometer) was used to perform the analysis. An energy dispersive spectrometer (EDS)-equipped Carl Zeiss/Gemini 300 scanning electron microscopy, (SEM) was used to analyze the morphological characteristics and chemical composition of CuCrZr powders and SLM samples. The Archimedes approach was utilized to analyze the relative density values of bulk samples produced via the SLM technology.

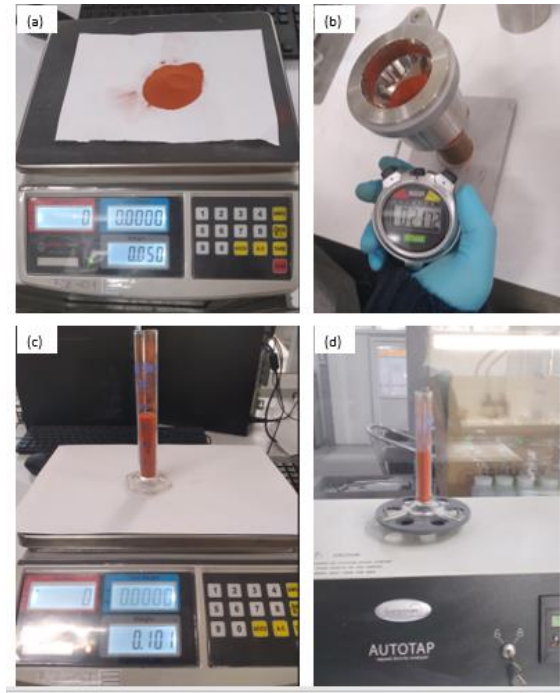


Figure 4. shows an image of powder density and flow ability tester equipment a) Copper powder b) Apparent density tester c) Graduated glass cylinder d) Compression density measurement device.

The process involved calculating the average of three weightings by measuring dry and wet weights in ethanol and air conditions Özkan *et al.* (2024), Tang *et al.* (2022) calculated the relative densities of the samples using a theoretical density of CuCrZr of 8.95 g/cm³. Samples were prepared for metallographic analysis using an ATM brand sanding and polishing tool and a Metkon Ecompress 100 brand mounting device. SiC grinding papers with grits of 400, 600, 800, 1200, and 2500 were used to sand all of the samples. Then, 1 μ m diamond suspensions were used to polish each sample to conduct a

metallographic examination on CuCrZr. The obtained bulk samples were examined microstructurally using an optical microscope (Nikon-Eclipse LV150N). Measurements of Vickers hardness were performed using a Qness Q10 microhardness tester for CuCrZr with 100gr and a dwell time of 15 seconds. Five measurements were taken for the hardness measurement from randomly selected regions in the sample, and the average of these values was computed.

The wear test parameters of CuCrZr, which were manufactured via the SLM technique, are shown in Table 2. To investigate the wear resistance of bulk samples, reciprocating dry wear tests were performed using 5 mm chrome steel balls in a BRUKERTM UMT2 tribometer according to ASTM E52100. A Leica stereo microscope was used to assess the wear volumes of bulk materials. The wear resistance of pure copper produced by SLM was examined for the first time by Aksa et al. (2022) and the test load, stroke, velocity and total distance were determined by taking into account this work and device capacity which was used in this study. The wear rate of CuCrZr was calculated using Eq. 2 (Aksa et al. 2022).

$$Wear\ rate\left(\frac{mm^3}{Nm}\right) = \frac{Wear\ volume\ (mm^3)}{Total\ wear\ distance(m)\times\ test\ load\ (N)} \quad (2)$$

Table 2. Wear test parameters of the search.

Test parameters	Values
Test type	Dry reciprocating
Test load (N)	3.5
Wear stroke (mm)	4
Velocity (mm/s)	7
Cycle	3750
Total distance (m)	30
Ball type	ASTM 52100 chrome steel balls
Temperature (C°)	Room temperature (23±2)

3. Results and Discussions

As shown in Table 3, According to the XRF analysis result, the powder composition complies with the EN 12420:2014 standard.

Table 3. Chemical composition of the CuCrZr alloy powder.

Element	Composition	EN 12420:2024
Cu	98.5	Rest
Cr	1.02	(0.5-1.2)
Zr	0.0779	(0.03-0.3)
Fe	0.0320	Max.(0.08)
Si	0.0428	Max.(0.1)
Others	< 0.3	-

Powder particle size results are shown in Figure 5 (a). Powder particle size is in the 24.4-50.8 µm range; it has

been determined that it is suitable for use in SLM. As seen in Figure 5 (b), XRD results of powder CuCrZr show the face-centered cubic microstructure. The diffraction peaks were found to be associated with the Cu phase. The (111), (200), and (220) planes of the face-centered Cu were identified as the source of the diffraction peaks at $2\theta = 43.24^\circ, 50.38^\circ, \text{ and } 74.03^\circ$ (Hu et al. 2023). Because of their low concentrations in the copper matrix, no peaks for the Zr and Cr particles were seen. Tang et al. (2022) and Ma et al. (2020) worked with CuCrZr powder by selective laser melting method in their study, and as stated in their study, the Cr and Zr elements in the powder could not be detected in the XRD analysis due to the small amount and limited device detection capacity (Tang et al. 2022), (Ma et al. 2020).

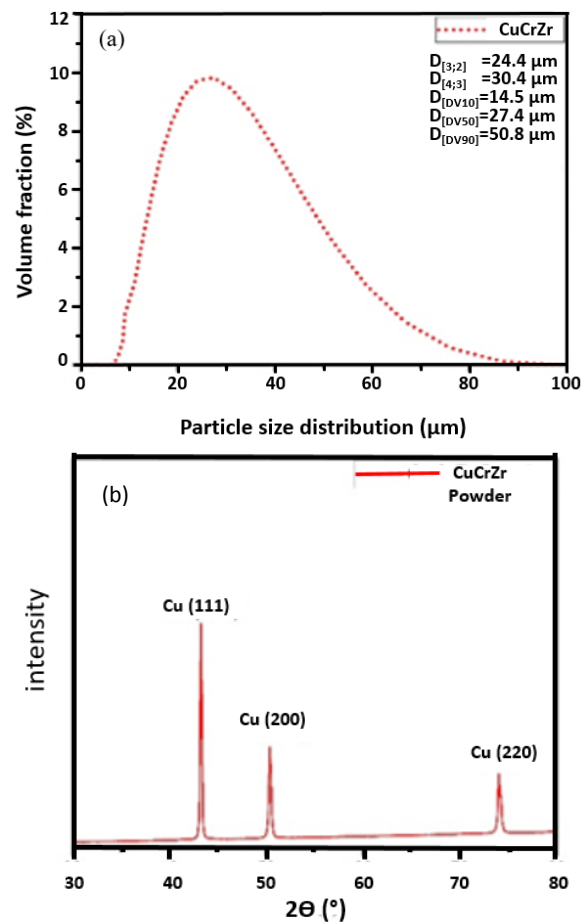


Figure 5. (a) Particle size distribution analysis result of CuCrZr powder (b) XRD patterns of the SLM CuCrZr powder.

SEM images of CuCrZr powder were shown in Figure 6 (a) 1000x image, b) 100x image. It can be seen that the powder particles have a smooth surface and spherical morphology, and some small particles are stuck to larger particles. It also has a good surface quality that positively affects fluidity. According to the SEM-EDS analysis given in Figure 7, Cr and Zr elements were detected in the Cu matrix. The analysis was made from the spectrum 1 region.

Figure 8 shows the microstructures of the samples produced with different parameters by the SLM method. All samples have non-circular and interconnected pores. As can be seen in Fig. 8 (a–e), the diameter of the porosities of the sample produced at the highest energy density (621.42 J/mm³) is smaller, and the shape of the porosities is more circular than the samples produced with a lower energy density (278.84 J/mm³). In this investigation, we obtained a similar relationship between porosity and energy density as a study by Zaneta (2019) on processing titanium with DMLS technology.

In their study they investigated the changes in porosity in the material caused by energy density. It's reported that porosity increased with the decrease in energy density. Low energy density (33–71 J/mm³) caused insufficient melting of powder grains, small laser penetration depth, and a small melt pool. It was observed that the porosity decreased significantly in the range of 78–127 J/mm³, and more spherical and smaller porosities emerged due to gas bubbles in the powder. This is explained the filling of voids between particulates with liquid. Also while the energy density above 127 J/mm³ the porosity was increased again (Zaneta 2019). Yunzhe et al (2024) studied on CuCrZr produced by EBM (electron beam melting) process and investigated the effect of the linear energy density on microstructure, nanoprecipitation, electrical and mechanical properties. It has been reported that low energy density results in low relative density, while high energy density results in microvoids.

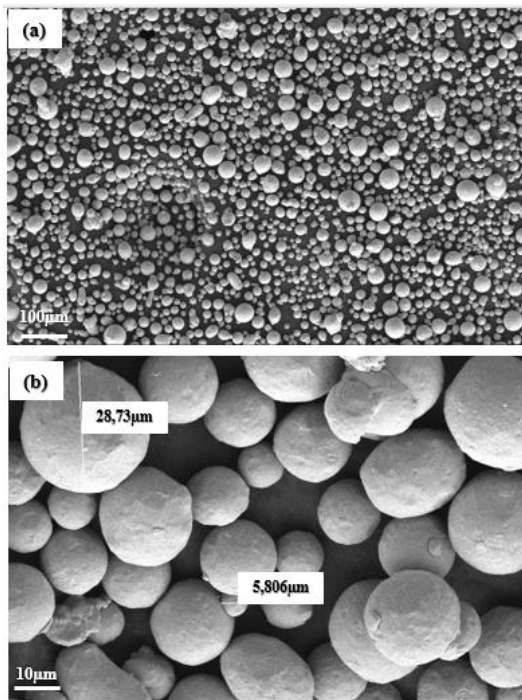


Figure 6. (a) shows 1000X, (b) 100X SEM images of CuCrZr powder.

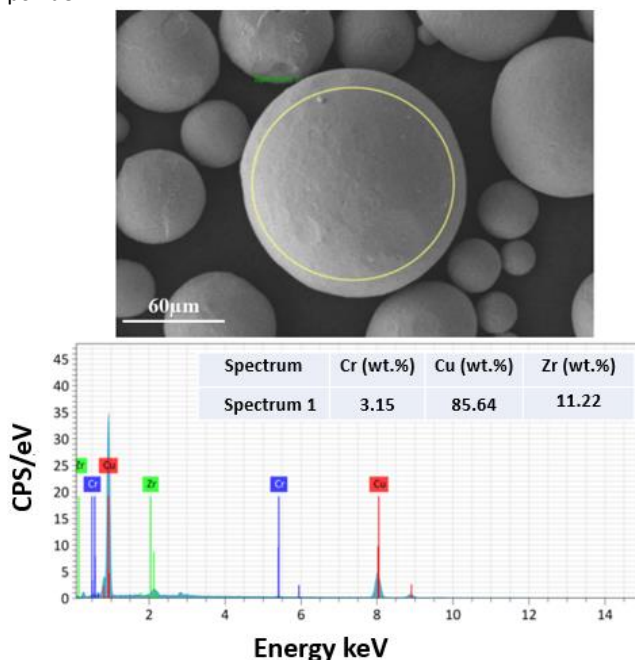


Figure 7. SEM-EDS results of CuCrZr powder

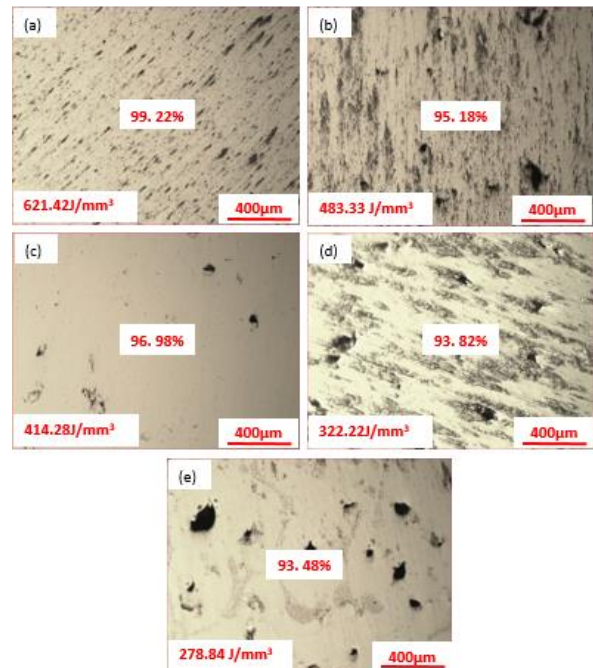


Figure 8. (a-e) shows 100X sample (1-5) optical microscope images of CuCrZr before etching respectively.

Fig. 9 (a-c) shows the microstructure of sample 1 after etching 100X, 200X, 1000X respectively. There are many spherical, regular, and small porosities in the microstructure. Grain boundaries are visible, and grain sizes were observed in the range of 6–120 µm.

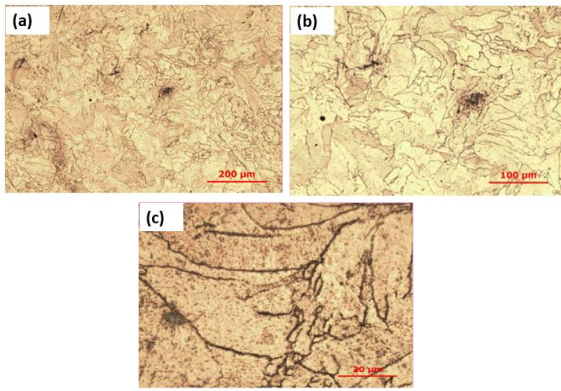


Figure 9. (a-c) shows sample 1 optical microscope images of CuCrZr after etching 100X, 200X, 1000X respectively.

Figure 10 show density value of fabricated sample with various parameters via SLM and results were obtained ranging from 93.48% to 99.22%. Xingchen *et al.*(2020) determined that the optimum linear energy density (laser power/laser scanning speed) was 0.50J/mm. And they observed in their study that as linear energy density increased, it increased in parallel with relative density and started to decrease after the peak point. In this study maximum relative density value %99.22 was obtained with optimum energy density as 621 J/mm³.

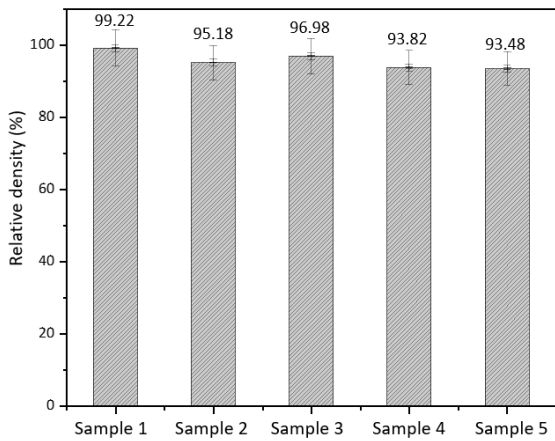


Figure 10. Relative density results of the study.

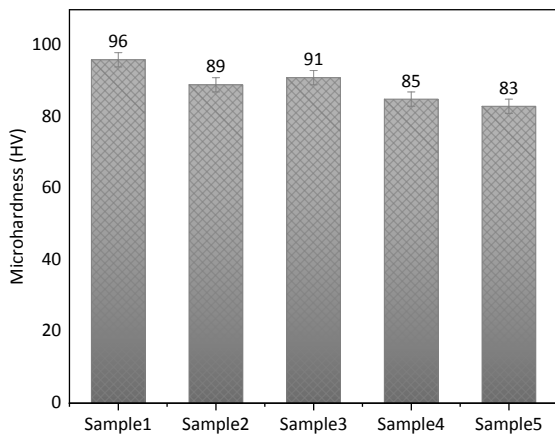


Figure 11. Microhardness of the SLM CuCrZr alloy.

Figure 11 shows the hardness test results of the CuCrZr samples. In this study, the highest microhardness value

and the highest density were obtained with sample 1. Hardness and density values in an alloy are mostly proportional to each other (Wang *et al.* 2022). In their study, researchers determined that the highest hardness value was at the optimum linear energy density and stated that this was due to fewer defects in the microstructure and higher relative density. And in their study, it was observed that the hardness was lower under the optimum energy density and decreased again after reaching the optimum value (Yan *et al.* 2020). The results show that the sample produced with the optimum energy density of 621J/mm³ has the highest hardness value and decreases in parallel with the energy density.

In the SLM process, as the CuCrZr powder melts at high temperatures and solidifies by rapidly cooling, a supersaturated solid solution that provides high strength is obtained, creating an effect similar to the solution heat treatment process (Wang *et al.* 2022). Wear test results are reported in Figure 12 and Table 4. At the beginning of the test, COF values increase and then become stable. The COF values were shown in Figure 12 and determined to be quite close to each other. The width and depth of the wear traces of the sample with the highest hardness and relative density and the sample with the lowest were obtained as close to each other as possible. The wear values of the CuCrZr sample are correlated by energy density, hardness, and relative density.

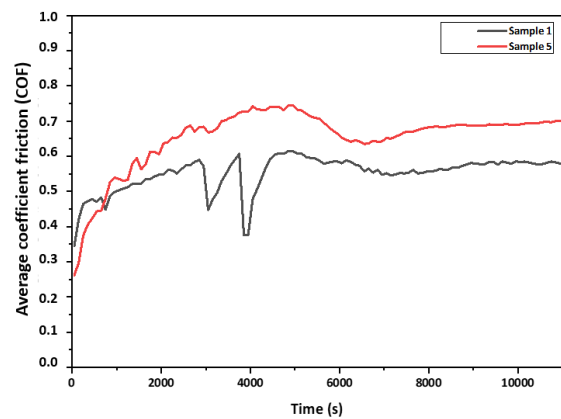


Figure 12. Average COF value of sample 1 and sample 5

Table 4. COF value of the CuCrZr via SLM process

Sample number	Average value	COF	Specific wear rate (mm ³ /Nm)
1	0.5520 ±0.1648		1.17 x 10 ⁻⁴
5	0.6536 ±0.2042		2.50 x 10 ⁻⁴

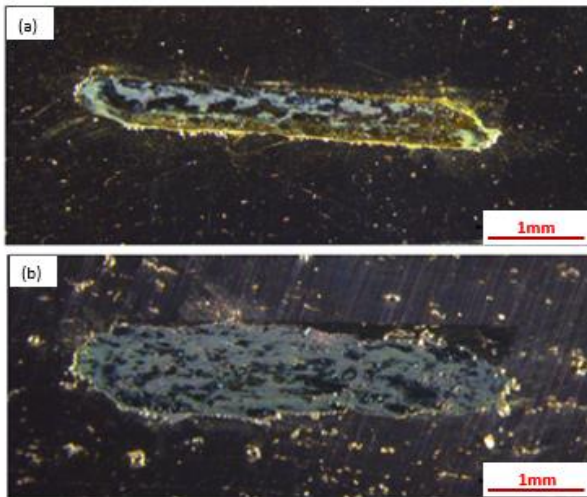


Figure 13. (a, b) Wear track image of SLM processed sample 1 and sample 5)

Stereomicroscope images of samples are shown in Fig.13. With a deeper and wider wear track image denser wear was seen in sample 5 than in sample 1. At the same time, it indicates higher wear volume and lower wear resistance through its wear volume loss value and wear profile. The higher hardness values of CuCrZr allow a higher level of wear resistance to the loads during the sliding test. Also, Figures 13 a) and b) show that the worn surface track image of sample 1 is wider than sample 5.

4. Conclusions

This study investigated the optimization of production parameters of domestically produced CuCrZr powder with the domestic SLM printer Ermaksan ENA 250 and the effect of process parameters on relative density, hardness, microstructure, and wear properties. CuCrZr alloy samples with different parameters were successfully fabricated via the SLM method. The optimum parameters were determined by revealing the density, hardness, and wear resistance results of the domestically produced CuCrZr powder samples processed by the SLM method.

Optimal process parameters for CuCrZr powder were determined. Energy density is 621.42 J/mm^3 , layer thickness is 0.02 mm, laser spot size is 0.1 mm, hatch distance is 0.1 mm, and laser power is 435 W, scanning speed is 350 mm/s. The relative density, hardness, COF value, and wear rate values of fabricated samples via optimal SLM process parameters were obtained as 99.22%, 95.88 HV, 0.5520 ± 0.1648 , and $1.17 \times 10^{-4} \text{ Nm}$, respectively. The highest relative density obtained with sample 1. It is predicted that at optimum energy density, the metallurgical bond between the layers is stronger, porosity and other defects are less, and therefore higher relative density and therefore higher hardness values are

achieved. As a result, the sample's hardness, density, and wear rate were obtained in direct proportion. The sample produced at the highest energy density has a smaller and more circular porosity diameter than the sample manufactured at a lower energy density, as seen by the optical microstructure images.

All samples have noncircular and interconnected pores. Considering the results, it can be said that when energy density is higher, porosity diameter is smaller, relative density is higher, hardness values are higher, and specific wear rate values are lower. As a result of this study, production with good mechanical properties has been successfully carried out via the domestically produced Ermaksan ENA 250 SLM printer using domestically produced CuCrZr powder. Future studies are planned to investigate the effect of heat treatment on mechanical properties.

Declaration of Ethical Standards

The authors declare that the article complied with all ethical rules

Credit Authorship/ Contribution Statement

Author 1: Investigation, Visualization and Writing, Methods, experimental design, Original draft

Author 2: Investigation, Methods, Experimental design, Writing

Author 3: Investigation, Methods, Experimental design

Author 4: Methods, Experimental design

Author 5: Method, Review and Editing

Author 6: Methods, Experimental design, Formal analysis, Review and Editing

Author 7: Methods, Experimental design, Project Manager, Review and Editing

Declaration of Competing Interest

There are no conflicts of interest, for the authors.

Data Availability Statement

All data generated or analyzed during this study are included in this published article.

Acknowledgement

This study was supported by "TUBITAK TEYDEB SAYEM Projects" with the project number of 121D022.

5. References

- Aksa, H.C., Hacısalihoğlu, İ., Yıldız, F., Varol, T., Güler, O., Kaya, G., 2022. Effects of Fabrication Parameters and Post-Processing Treatments on the Mechanical and Tribological Behavior of Surface-Enhanced Copper Based Materials by Selective Laser Melting. *Journal of Materials Processing Technology*, **304**, 117564. <https://doi.org/10.1016/j.jmatprotec.2022.117564>

- Fank, X., Xia, W., Wei, Q., Yiping, W., Lv, W., Guo, W. 2021. Preparation of Cu-Cr-Zr Alloy by Laser Powder Bed Fusion: Parameter Optimization, Microstructure, Mechanical and Thermal Properties for Microelectronic Applications. *Metals*. **11**(9), 1410. <https://doi.org/10.3390/met11091410>
- Frazier, W. E. 2014., 2024. Metal Additive Manufacturing: A Review. *Journal of Materials Engineering and Performance* **23** (6): 1917–28. <https://doi.org/10.1007/s11665-014-0958-z>
- Gokuldoss, P. K., Kolla S., and Eckert J., 2017. Additive Manufacturing Processes: Selective Laser Melting, Electron Beam Melting and Binder Jetting—Selection Guidelines. *Materials* **10** (6): 672. <https://doi.org/10.3390/ma10060672>
- Hu, R., Su, K., Lao, Z., Cai, Y., Fu, B., Yuen, M.M F, Gao Z, Cao M, and Wang, Y., 2023. Process of Pure Copper Fabricated by Selective Laser Melting (SLM) Technology under Moderate Laser Power with Re-Melting Strategy. *Materials* **16** (7): 2642. <https://doi.org/10.3390/ma16072642>
- Ma, Z., Zhang, K., Ren, Z., Zhang, D., Tao, G., Xu, H., 2020. Selective laser melting of CuCrZr copper alloy: Parameter optimization, microstructure and mechanical properties. *Journal of Alloys and Compounds* **828** (February) 154350. <https://doi.org/10.1016/j.jallcom.2020.154350>
- Murugesan S.K., Natarajan J., Yang C.H., 2024. Enhancing the wear resistance by mitigation of defect formations in laser powder bed fusion process of Cu–Cr–Zr alloy. *The International Journal of Advanced Manufacturing Technology*. **133**:1845–1864. <https://doi.org/10.1007/s00170-024-13883-3>
- Özkan, B., Dilsiz, Y., Küçükelyas, B., Sever, A., Bademlioglu, A.H., Kaboğlu, C., and Uzunsoy, D. 2024., Comprehensive Optimization of Selective Laser Melting Process Parameters for Microstructure, Density, Hardness, and Tribological Performance of Pure Copper. *Science of Sintering*. **56** 349–365 <https://doi.org/10.2298/SOS2402150070>
- Prabu, G., Yang, C.H., Alnaser, İ.A., and Jeyaprakash, N., 2024. Nanowear Characterization of LPBF Fabricated CuCrZr Alloy. *Tribology International* **194** (June): 109430. <https://doi.org/10.1016/j.triboint.2024.109430>
- Prashanth, K.G., Scudino S., Klaus H.J, Surreddi K.B, Löber L., Wang Z, Chaubey A.K., Kühn U., and Eckert J., 2014. Microstructure and Mechanical Properties of Al–12Si Produced by Selective Laser Melting: Effect of Heat Treatment’. *Materials Science and Engineering: A* **590** (January): 153–60. <https://doi.org/10.1016/j.msea.2013.10.023>
- Raab, S, J., Guschlbauer R., Lodes M.A., and Körner C., 2016. Thermal and Electrical Conductivity of 99.9% Pure Copper Processed via Selective Electron Beam Melting. *Advanced Engineering Materials* **18** (9): 1661–66. <https://doi.org/10.1002/adem.201600078>
- Salvan, C., L. Briottet, T. Baffie, L. Guetaz, and C. Flament., 2022. CuCrZr Alloy Produced by Laser Powder Bed Fusion: Microstructure, Nanoscale Strengthening Mechanisms, Electrical and Mechanical Properties. *Materials Science and Engineering: A* **826** (October): <https://doi.org/10.1016/j.msea.2021.141915>
- Sun, F., Liu P., Chen X., Zhou H., Guan P., and Zhu B., 2020. Mechanical Properties of High-Strength Cu–Cr–Zr Alloy Fabricated by Selective Laser Melting *Materials* **13** (21): 5028. <https://doi.org/10.3390/ma13215028>
- Tang, X., Chen, X., Sun, F., Li, L., Liu, P., Zhou, H., Fu, S and Li. A., 2022. A Study on the Mechanical and Electrical Properties of High-Strength CuCrZr Alloy Fabricated Using Laser Powder Bed Fusion’. *Journal of Alloys and Compounds* **924** (November): 166627. <https://doi.org/10.1016/j.jallcom.2022.166627>
- Wang, Q., Zhang, Y., Wang, K., Liu, S., Zhang, X and Shao H., 2022. Effect of Process Parameters and Heat Treatment on the Microstructure and Properties of CuCrZr Alloy by Selective Laser Melting’. *Materials Science and Engineering: A* **857**: 144054. <https://doi.org/10.1016/j.msea.2022.144054>
- Xu L., Zhang, Y., Zhao, L., Ren, W and Han, Y., 2024. Performance Improvement for the CuCrZr Alloy Produced by Laser Powder Bed Fusion Using the Remelting Process. *Materials* **17** (3): 624. <https://doi.org/10.3390/ma17030624>
- Yang X., Chang C.C., Dong D., Gao S., Ma W., Liu M., Liao H., Yin S., 2020. Microstructure and mechanical properties of pure copper manufactured by selective laser melting. *Materials Science & Engineering A* **789** 139615. <https://doi.org/10.1016/j.msea.2020.139615>
- Yaolong, C., Qiang, H., Linshan, W., Wenqian, G., and Jinhui, Z., 2024. Study on Densification and Defects of Cu-Cr-Zr Alloy Formed by Selective Laser Melting. *Journal of Physics: Conference Series* **2785** 012139. <https://doi.org/10.1088/1742-6596/2785/1/012139>
- Yap, C. Y., Chua, C. K., Dong, ZL., Liu, ZH., Zhang, D. Q., Loh, L.E., Sing, SL., 2015. Review of Selective Laser Melting: Materials and Applications’. *Applied Physics Reviews* **2** (December): 041101. <https://doi.org/10.1063/1.4935926>
- Yunzhe L., Shifeng L., Yan W., Jianyong W., Liangliang Z., Ping Y., Wenbin W., 2024. Effect of electron beam energy density on the microstructure and properties of CuCrZr alloy prepared by electron beam powder bed fusion (EB-PBF), *Materials Characterization*. 214 114031. <https://doi.org/10.1016/j.matchar.2024.114031>

Zaneta A. M., 2019. Effect of Laser Energy Density, Internal Porosity and Heat Treatment on Mechanical Behavior of Biomedical Ti6Al4V Alloy Obtained with DMLS Technology,. *Materials*, **12**, 2331.
<https://doi.org/10.3390/ma12142331>

Ze Zhou K, Li Z, Liu B, Chen Y, Li H, and Bai P., 2023. Microstructure and Mechanical Properties of CuCrZr/316L Hybrid Components Manufactured Using Selective Laser Melting'. *Journal of Alloys and Compounds* **955** (September): 170103.
<https://doi.org/10.1016/j.jallcom.2023.170103>

Zhangping, H., Zunfeng, D., Zhenwen, Y., Liming, Y., Zongqing, M., 2022. Preparation of Cu–Cr–Zr alloy by selective laser melting: Role of scanning parameters on densification, microstructure and mechanical properties *Materials Science & Engineering A* **836** 142740.
<https://doi.org/10.1016/j.mesa.2022.142740>